Structure of a DNA Duplex That Contains α-Anomeric Nucleotides and 3′−3′ and 5′−5′ Phosphodiester Linkages: Coexistence of Parallel and Antiparallel DNA†

James M. Aramini,‡ Bernd W. Kalisch,§ Richard T. Pon,§ Johann H. van de Sande,§ and Markus W. Germann*,‡

Department of Pharmacology, Kimmel Cancer Institute, Thomas Jefferson University, Philadelphia, Pennsylvania 19107, and Department of Medical Biochemistry, University of Calgary, Calgary, Alberta, Canada T2N 4N1

Received March 12, 1996; Revised Manuscript Received May 8, 1996⊗

ABSTRACT: We report a comparative spectroscopic study of a novel self-complementary duplex decamer, d(GCGAAT-3′-3′-(αT)-5′-5′-CGC)$_2$, in which an α-anomeric nucleotide has been inserted into the sequence in a parallel orientation via 3′−3′ and 5′−5′ phosphodiester bonds, and its unmodified B-DNA analog, d(GCGAATTCGC)$_2$. Plots of the hyperchromicity and circular dichroism of these oligonucleotides are virtually identical, indicating that the overall base stacking and handedness are preserved in the α duplex. Thermodynamic parameters extracted from UV melting experiments show that the α duplex is only slightly less stable than the control. A near complete set of ^{1}H and ^{31}P nuclear magnetic resonance (NMR) assignments were obtained for both duplexes using classical one- and two-dimensional approaches. Several lines of evidence, in particular, imino ^{1}H, ^{31}P, nuclear Overhauser enhancement, and deoxyribose ring proton spin−spin coupling data, convincingly demonstrate that the overall structural integrity of the α and control duplexes are quite comparable, with any perturbations in the former localized to the regions of the construct encompassing the α-nucleotide and the unique backbone linkages. Specifically, the α duplex exhibits normal Watson−Crick type base pairing, it remains antiparallel except at the inverted nucleotide, all bases are in the anti orientation, and the sugar ring puckering is predominantly "S"-type. However, the *J*-coupling information for the α-nucleotide and the neighboring (3′) cytidine are notably different, and reflect a decrease in the amplitude of the sugar pucker in αT7, and a significant shift in the conformational equilibrium of the furanose ring in C8 toward the "N"-type pucker. The feasibility of synthesizing oligodeoxynucleotides containing a combination of α sugars and short parallel stranded segments, their propensity for forming stable duplexes, and the structural insights into such complexes reported here are of potential importance in the area of antisense therapy.

The potential of manipulating gene expression with both high selectivity and affinity has led to considerable interest into antisense DNA[1] therapy, with the ultimate goal of revolutionizing the treatment of a broad spectrum of diseases (recently reviewed by: Crooke, 1993; Stein & Cheng, 1993; Hélène, 1994; Wagner, 1994). The basic strategy involves the design of an "antisense" oligodeoxynucleotide which binds in a specific fashion to a "sense" messenger RNA sequence whose gene product is *a priori* known to be involved in the etiology of the disease. The desired inhibition of mRNA translation may then be accomplished in a number of ways, such as RNase H cleavage of the mRNA strand in the resulting RNA−DNA hybrid. Although the mechanism of action of, and cellular response to, such reagents is not clearly understood, several traits have been deemed crucial for their efficacy, in particular, cellular uptake and stability (i.e., resistance to endogenous nucleases). In this vein, a great deal of attention has been focused on the development of sequences containing a variety of unnatural moieties, especially involving modifications to the phosphodiester backbone; two promising examples are the phosphorothioates (the first generation of antisense drugs to reach clinical trials) and methyl phosphonates (Milligan et al., 1993; de Mesmaeker et al., 1995).

Beginning in the late 1980s, research into the applicability of the synthetically less demanding α-containing deoxynucleotides as antisense agents established (1) their ability to form relatively stable hybrids with complementary β-DNA and β-RNA sequences (i.e., Prasueth et al., 1987; Thuong et al., 1987; Paoletti et al., 1989) and (2) their resistance to nuclease degradation (Vichier-Guerre, 1994, and references therein), although these properties are somewhat sequence dependent. Several investigations have demonstrated the ability of α-DNA strands to inhibit mRNA translation in cell-free extracts in an RNase H-independent manner (Bertrand et al., 1989; Boiziau et al., 1991, 1992), as well as viral growth (Lavignon et al., 1992; Jacob et al., 1993; Zelphati et al., 1994). Recently, the antisense potential of α-β chimeric oligonucleotides, in which the α and β sequences are fused together by a 3′−3′ phosphodiester linkage, was illustrated by their involvement in RNase H-mediated arrest

† This work was supported by a grant from the Natural Sciences and Engineering Research Council of Canada (J.H.v.d.S.).

* To whom correspondence should be addressed: Tel: (215) 503-4581; FAX: (215) 923-2117; E-mail: mwg@bern.jci.tju.edu.

‡ Thomas Jefferson University.

§ University of Calgary.

⊗ Abstract published in *Advance ACS Abstracts,* June 15, 1996.

[1] Abbreviations: 1D, one dimensional; 2D, two dimensional; BSA, bovine serum albumin; CD, circular dichroism; DEAE, (diethylamino)-ethane; DNA, deoxyribonucleic acid; DQF-COSY, double quantum filtered correlated spectroscopy; DMT, dimethoxytrityl; DSS, 2,2-dimethylsilapentane-5-sulfonate; DTT, dithiothreitol; EDTA, ethylene-diaminetetraacetic acid; FID, free induction decay; HPLC, high performance liquid chromatography; NMR, nuclear magnetic resonance; NOE, nuclear Overhauser enhancement; NOESY, NOE spectroscopy; RNA, ribonucleic acid; TOCSY, total correlated spectroscopy; TPPI, time proportional phase increment; Tris, tris(hydroxymethyl)aminomethane; UV, ultraviolet.

S0006-2960(96)00612-5 CCC: $12.00

of reverse transcription *in vitro* (Boiziau et al., 1995). Moreover, it has been recently demonstrated by gel electrophoresis and UV denaturation studies that α-*β* chimeric oligodeoxynucleotides containing multiple polarity reversals, which were generated by a combination of 3′−3′ and 5′−5′ phosphodiester bonds, can form stable duplexes with complementary DNA and RNA sequences (van de Sande et al., 1994; Kalisch et al., unpublished results; Koga et al., 1995). Alternating 3′−3′ and 5′−5′ phosphodiester moieties flanking each α-nucleotide enable these residues to effectively participate in base pairing and base stacking. In such constructs, duplex stability and nuclease resistance increase with increasing number of polarity reversals and α content at the expense of RNase H sensitivity. Hence, the amount of *β*-nucleotides and natural phosphodiester linkages must be chosen judiciously so as to ensure duplex formation with the target RNA, yet allow hydrolysis of the hybrid duplex by RNase H.

The need to shed light on the structural aspects of complexes containing α-deoxynucleotides at a molecular level led to a number of NMR studies on short α-DNA/*β*-DNA hybrids, which provided evidence for the formation of stable *parallel* right-handed duplexes, containing Watson−Crick base pairing, anti-glycosidic linkages, and predominantly S-type sugar ring puckering in both strands (Morvan et al., 1987; Lancelot et al., 1987, 1989; Guesnot et al., 1990). Subsequent reports on a decamer hybrid α-d(CGCAATTCGC)-*β*-(GCGTTAAGCG) and a short α-DNA/*β*-RNA hybrid corroborated these findings (Gmeiner et al., 1990, 1992).

The ability of nucleic acids to form stable parallel structures under various conditions has established the parallel stranded motif as another of the alternative structural forms, aside from the classical B-type, in which DNA can exist (Rippe & Jovin, 1992; Germann et al., 1995). Investigations into a number of DNA hairpins have demonstrated that unusual phosphodiester linkages (i.e., 5′−5′ and 3′−3′) can force the stem to adopt a parallel configuration, featuring reverse Watson−Crick base pairing between the complementary strands (van de Sande et al., 1988, 1990; Germann et al., 1989; Zhou et al., 1993).

The objective of this work was to use a combination of the α-anomeric nucleotide and 5′−5′ and 3′−3′ phosphodiester linkage approaches to synthesize a novel self-complementary DNA decamer, d(GCGAAT-3′-3′-(αT)-5′-5′-CGC). Model building studies in our laboratory suggest that, despite these modifications, this construct should accommodate a regular antiparallel double helical structure, with one nucleotide in a parallel alignment in each strand. In this paper, we compare the structural and thermodynamic properties of this α-containing duplex decamer to those of a control B-DNA duplex containing the same sequence d(GCGAATTCGC). We will demonstrate that the αT decamer can indeed form a stable duplex, whose structure is not greatly perturbed from that of the control.

EXPERIMENTAL PROCEDURES

Synthesis and Purification. α-D-Thymidine was purchased from Sigma Chemical Co.; all other reagents used in the synthetic work were obtained from Aldrich Chemical Co. The 5′-phosphoramidite of αT required for the synthesis of the αT decamer was prepared from the α-anomeric nucleoside according to the following three-step protocol (shown in Figure 1A):

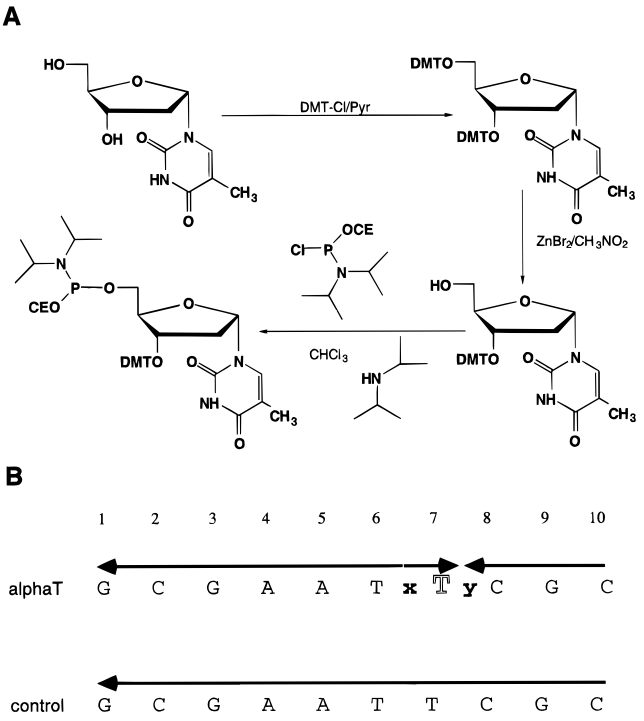

FIGURE 1: (A) Synthesis of 5′-phosphoramidite-3′-DMT derivative of α-anomeric thymidine used for preparation of the αT decamer. (B) Sequences of the αT and control decamers used in this study; x and y denote the 3′−3′ and 5′−5′ phosphodiester linkages, respectively; the α-anomeric thymidine is outlined.

(*1*) *Preparation of 3′,5′-Bis(dimethoxytrityl)-α-thymidine*. α-Thymidine (4 mmol, 968 mg) was coevaporated to dryness with anhydrous pyridine (3×). The nucleoside was redissolved in pyridine (50 mL) and dimethoxytrityl chloride (10 mmol, 3.4 g) was added. After stirring overnight at room temperature, the reaction was concentrated to half volume by evaporation and redissolved in $CHCl_3$ (100 mL). The solution was washed with $NaHCO_3$ (3 × 50 mL) and water. The crude product was purified by silica gel chromatography (5% MeOH/$CHCl_3$) to yield the pure product as a light yellow foam (80% yield).

(*2*) *Preparation of 3′-(Dimethoxytrityl)-α-thymidine*. 3′,5′-Bis(dimethoxytrityl)-α-thymidine (2.4 mmol, 2 g) was dissolved in nitromethane (60 mL), cooled on ice, and added to a suspension of zinc bromide (10 mmol, 2.3 g) in nitromethane. After stirring (0 °C, 2 h), 1 M aqueous ammonium acetate (100 mL) was added. The reaction was washed with $CHCl_3$ (1 × 100 mL), and the organic phase was washed with water (3×). The crude product was purified by silica gel chromatography (5% MeOH/$CHCl_3$) to give the pure product as a white foam (60% yield).

(*3*) *Preparation of 3′-(Dimethoxytrityl)-α-thymidine 5′-(2-Cyanoethyl-N,N-diisopropylphosphoramidite)*. Anhydrous diisopropylamine (5.3 mmol, 0.7 mL), and 3′-(dimethoxytrityl)-α-thymidine (1.6 mmol, 0.87 g) were dissolved in anhydrous $CHCl_3$ (15 mL) in a septum scaled flask. 2-Cyanoethyl *N,N*-diisopropylchlorophosphoramidite (1.6 mmol, 357 μL) was added via syringe. After stirring (room temperature, 2 h), the reaction was washed with aqueous NaCl (1 × 15 mL) and then water (3 × 20 mL). The $CHCl_3$ solution was concentrated to ≈3 mL and applied directly to a silica gel column prepared and equilibrated in 42:55:3 CH_2-

Cl_2/hexane/triethylamine. Elution with this same solvent mixture yielded the pure product as a white foam (80% yield).

The αT decamer, d(GCGAAT-3′-3′-(αT)-5′-5′CGC), was prepared in two simultaneous 15 μmol scale syntheses using an Applied Biosystems 380B DNA synthesizer. The αT phosphoramidite was used at a 0.1 M concentration in the same manner as that for the standard phosphoramidite reagents in a large scale synthesis cycle. After cleavage from the support, the 5′-detritylated product in NH_4OH was heated (55 °C, 16 h) to complete the deprotection. After evaporation of the NH_4OH, the crude product was redissolved in water and desalted on a Sephadex G-25 column (1.6 cm × 40 cm). Aliquots (≈250 A_{260} units) were purified by HPLC using a Waters DEAE-5PW anion exchange column (2.25 cm × 15 cm) with a gradient elution (0−16% 1 M $NaClO_4$, 0−90 min, 5 mL/min). The purified product was collected, concentrated, and desalted on Sephadex G-25. Total yield was 675 A_{260} units (≈24 mg) of product, 90−95% pure. The control decamer, d(GCGAATTCGC), was synthesized and purified by reverse-phase HPLC on a PRP-1 column as previously described (Germann et al., 1987). Preparations of both decamers for T_m studies were synthesized as above on a 1 μmol scale and were purified by preparative 24% polyacrylamide gels (8 M urea, 90 mM Tris−borate, 5 mM EDTA, pH 8.3).

5′ End-Labeling. Oligonucleotides were 5′ end-labeled with a 2-fold excess of [γ-^{32}P]ATP and T_4 polynucleotide kinase in 10 mM $MgCl_2$, 5 mM DTT, and 50 mM Tris, pH 7.6, 37 °C, for 30 min (Chaconas & van de Sande, 1980). Reactions were terminated by heat inactivation of the enzyme (95 °C; 5 min) and subsequently purified by preparative gel electrophoresis on a 15% polyacrylamide gel (90 mM Tris−borate, 5 mM EDTA, pH 8.3).

Restriction Enzyme Reactions. Oligonucleotides were digested for 1 h at 32 °C with *Eco*RI (6 units/pmol of substrate) under standard conditions (100 mM NaCl, 10 mM $MgCl_2$, 100 μg/mL BSA, 1 mM β-mercaptoethanol, 10 mM Tris, pH 7.5). The 5′ end-labeled products of the *Eco*RI digestion were analyzed by denaturing gel electrophoresis on 15% polyacrylamide gels (8 M urea, 90 mM Tris−borate, 5 mM EDTA, pH 8.3). Kodak-X-Omat 5 film was used for autoradiography.

Optical Spectroscopy. Ultraviolet (UV) absorption spectra and thermal denaturation profiles were recorded on a Varian CARY 3E spectrophotometer equipped with thermostated cuvette holders. Molar extinction coefficients were calculated from the absorbance for this sequence under denaturing conditions (ϵ_{260} = 104 260 M^{-1} cm^{-1} in 5.0 M $NaClO_4$, 90 °C, pH 7.2) based on the mononucleotide contribution under identical conditions. Duplex concentrations were calculated using the hyperchromicity at 260 nm under the appropriate conditions (see legends to figures and tables for duplex and salt concentrations used in all spectroscopic experiments presented here). Hyperchromicity profiles were obtained by dividing the absorbance of the denatured forms (85 °C) by that of the double helical forms (5 °C). Circular dichroism spectra were recorded on a Jasco J-500C spectropolarimeter interfaced to a 386PC. The thermal denaturation of the duplexes was followed at 260 or 275 nm, and the temperature was increased at 0.4 °C/min. In each case, absorbance readings were collected at 0.2 deg intervals, and were fitted to a two-state (helix ↔ coil) model to yield the enthalpy of formation of the duplex, $\Delta H°$, and the melting temperature, T_m, as described previously (Germann et al., 1988). Briefly, a six-parameter fit was utilized which contained the temperature-dependent absorbance of helix and coil forms. Entropies were calculated from $\Delta H°$ and T_m (in K) using:

$$\Delta S° = \frac{\Delta H°}{T_m} - R \ln(C_T/4) \quad (1)$$

where C_T is the total strand concentration. Thermodynamic parameters were also calculated from the concentration dependence of the melting temperature (Cantor & Schimmel, 1980; Germann et al., 1988).

NMR Spectroscopy. Samples for NMR spectroscopic analysis were prepared by dissolving the lyophilized powder in 0.3−0.4 mL of buffer (10 mM Na_2HPO_4, 50 mM NaCl, 0.1 mM EDTA, pH 6.5). For the initial imino proton work, the solvent was 90% H_2O/10% D_2O; the samples were subsequently exchanged into D_2O (a minimum of two freeze−thaw cycles) for studies of the nonlabile protons and ^{31}P NMR.

All NMR experiments were performed on a Bruker AMX 600 NMR spectrometer equipped with a 5 mm broadband inverse probe, at ^{1}H and ^{31}P frequencies of 600.1 and 242.9 MHz, respectively, using the XWINNMR 1.0 software package run on a Silicon Graphics INDY work station. 1D ^{1}H NMR spectra of samples in D_2O were typically acquired with a total repetition time of 2.7−3.8 s and presaturation of the residual HDO signal during the delay time. 1D imino proton NMR spectra were obtained using the 1−1 jump and return technique (Plateau & Guéron, 1982), where the water signal is positioned at the center of the spectrum, and with a delay of 50 μs between phase-shifted pulses to optimize the desired signals; a total repetition time of 1.4 s was used. All 1D ^{1}H NMR data were transformed with a 0.3−1 Hz exponential line broadening. Phase-sensitive 2D NOESY spectra of the decamers in D_2O were acquired using the TPPI method (Marion & Wüthrich, 1983) under the following conditions: 2K data points in t_2, 512 experiments in t_1 with 24 scans per increment, a total repetition time of 5.2 s, and presaturation of the residual HDO signal. Phase-sensitive DQF-COSY experiments on the duplexes in D_2O were acquired using TPPI as well as the phase cycling scheme of Derome and Williamson (1990). Typical acquisition parameters are as follows: 2K data points in t_2, 1600 experiments in t_1 with 16 scans per increment, a total repetition time of 2.2 s, and presaturation of the residual HDO signal. NOESY and DQF-COSY data were processed with 90° shifted sine bell functions in both dimensions followed by automatic baseline correction in F1 and F2. Longitudinal (T_1) relaxation times for the adenosine H2 protons were determined by the inversion recovery technique ($\pi-\tau-(\pi/2)-$FID). All ^{1}H chemical shifts reported in this paper are with respect to internal DSS.

1D ^{31}P NMR spectra were acquired using the following parameters: a 70° pulse length, a 4900 Hz sweep width, 4K data points, and a repetition time of 2.4−3.8 s. The raw data were zero-filled to 8K, and a 1 Hz exponential line broadening was applied prior to Fourier transformation. All ^{31}P NMR spectra are referenced to 85% H_3PO_4 in an external capillary.

Other experiments, including 1−1 NOESY (Sklenar & Bax, 1987), TOCSY (Bax & Davis, 1985), and ^{1}H detected

$^{1}H-^{31}P$ correlation spectroscopy (Sklenar et al., 1986), were used to assist in assignment and are not presented in this paper.

Molecular Modeling. Models were manipulated using the molecular modeling software QUANTA (Molecular Simulations Inc.). The initial model was based on the PDB coordinates of the Dickerson dodecamer DNA duplex (Westhof, 1987); both 5′ and 3′ terminal base pairs were removed. The duplex containing the α-anomeric T was derived from the decamer duplex according to the following procedure. First, the chirality of the C1′ atom of T7 was modified to obtain the α anomeric form. Subsequently, the 5′ and 3′ O−P bonds of the αT nucleotide were broken, and the residue was rotated by 180° orthogonal to the helical axis. The residue was positioned for Watson−Crick base pairing and the O−P bonds were regenerated. The resulting structure was optimized with AMMP run on a Pentium PC under Windows 3.1 using no cutoff for nonbonded interactions (Harrison, 1993; Harrison & Weber, 1994). The minimizations were typically accomplished in a few minutes. The unusual linkages were readily generated in AMMP using the sp2 modification of the UFF force field (Weber & Harrison, 1996). The dielectric constant was set to 1; charges were based on the AMBER force field (Weiner et al., 1986). No explicit hydrogen bonds were added. Initially, only the αT nucleotide was minimized to overcome poor starting geometries, followed by the αT-A base pair, and finally the entire duplex structure (RMSF <4 kJ mol^{-1} Å^{-1}).

RESULTS AND DISCUSSION

Rationale and Design. Previous experiments have demonstrated that oligodeoxynucleotides containing exclusively α-anomeric nucleotides hybridize in a *parallel* stranded orientation with either *β*-DNA or *β*-RNA. This behavior was predicted years ago by Séquin (1973), who also postulated that the incorporation of an α-anomeric component in an otherwise fully *β*-anomeric DNA duplex would result in a significantly destabilized duplex, by reasoning that the base in the α-nucleotide cannot participate in base pairing within an antiparallel environment (Séquin, 1973). In our earlier work on parallel stranded duplex DNA, we employed 3′−3′ and 5′−5′ phosphodiester linkages to encourage the formation of parallel stranded DNA in the absence of any sequence constraints (van de Sande et al., 1988). In this study, we use these linkages to invert the strand polarity and provide an α-anomeric base with a local parallel stranded environment (see Figure 1B). This should enable it to participate in base pairing and base stacking and therefore contribute to the duplex stability. Thus, the αT duplex contains a novel feature in that it has parallel segments (one in each strand) embedded in an overall antiparallel helix.

Gel Electrophoresis and UV and CD Spectroscopy. The control and αT decamers were analyzed by gel electrophoresis under native conditions (Figure 2). Both sequences are self-complementary and have the intrinsic potential to form hairpin (i.e., unimolecular) structures, as was noted previously for analogous decamer and dodecamer sequences also containing the *Eco*RI consensus sequence (Marky et al., 1983; Rinkel et al., 1987b). Indeed, both decamers exhibit hairpin formation at low concentration (0.5 μM), with mobilities similar to that of a control duplex with 4 CG base pairs. Inspection of the gel reveals that the α decamer has

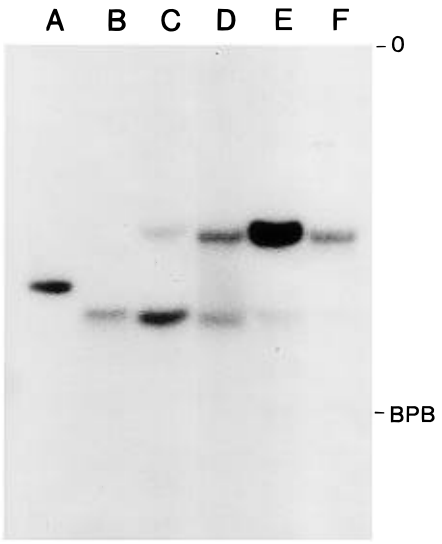

FIGURE 2: Gel electrophoretic analysis of hairpin-dimer formation for the control and αT decamers under native conditions (15% polyacrylamide, 90 mM Tris−borate, 15 mM $MgCl_2$, pH 8.3, 5 °C). Lane A, dT_{11} marker; lane B, $d(CCGG)_2$ (300 μM); lane C, $d(GCGAAT\text{-}3'\text{-}3'\text{-}(\alpha T)\text{-}5'\text{-}5'\text{-}CGC)_2$ at low concentration (0.5 μM); lane D, $d(GCGAATTCGC)_2$ at low concentration (0.5 μM); lane E, $d(GCGAAT\text{-}3'\text{-}3'\text{-}(\alpha T)\text{-}5'\text{-}5'\text{-}CGC)_2$ at high concentration (115 μM); lane F, $d(GCGAATTCGC)_2$ at high concentration (115 μM). All samples were fully phosphorylated; the low and high concentration decamer samples, with the exception of lane E, contain the same amount of ^{32}P label; the sample in lane E contained 4 times the amount of label to improve the detection of the hairpin form. The samples were applied in TBM buffer containing 10% glycerol; prior to loading, all samples were heated to 90 °C (0.5 min) and allowed to cool slowly to room temperature (30 min). The values in parentheses above are the strand concentrations of the oligonucleotides applied to the gel. BPB, bromophenol blue; O, origin.

a higher propensity for forming hairpin structures (>80%) than the control decamer (<30%), due to the presence of the α-anomeric nucleotide near the center of the sequence; this, consequently, destabilizes the duplex compared to the hairpin. However, at higher concentrations (115 μM) the duplex forms are highly favored for both sequences (i.e., no hairpin form is detectable for the control and <2% for the αT decamer). No bands due to higher order structures could be detected under the gel electrophoretic conditions.

Hyperchromicity profiles are very sensitive to the stacking interaction and assist in defining the strand disposition in parallel and antiparallel DNA with identical base composition (Germann et al., 1988; Ramsing & Jovin, 1988). Such profiles are a global indicator of the stacking interactions in a double helix. The hyperchromicity profiles of the control and αT duplexes are virtually identical in magnitude as well as peak position for both low and high strand concentrations (Figure 3A). These profiles differ from those obtained for antiparallel (or parallel) sequences containing exclusively AT base pairs, as may be expected because of the different base composition. The rather remarkable similarity of the hyperchromicity profiles indicates that the α-containing duplex is fully base paired in 400 mM NaCl and that the stacking interactions are very similar to those of the control decamer. Further evidence in favor of this is obtained from the CD spectra of these duplexes under native and denaturing conditions (Figure 3B). Both native spectra are very similar, are diagnostic of an overall right-handed B-type helical structure, and are comparable to spectra obtained at high concentrations (Figure 3C). These experiments indicate that

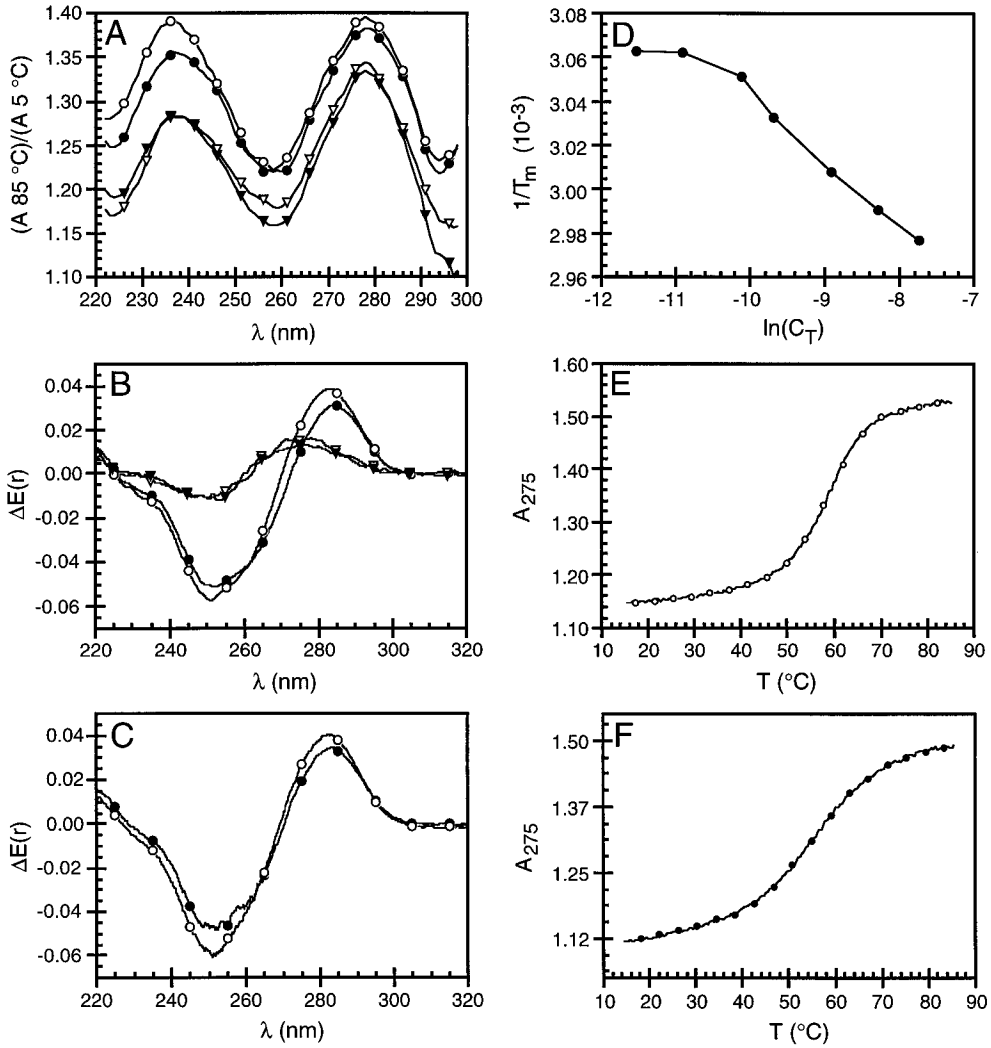

FIGURE 3: Hyperchromicity, circular dichroism, and melting curves for d(GCGAATTCGC)$_2$ and d(GCGAAT-3′-3′-(αT)-5′-5′-CGC)$_2$ each recorded in 400 mM NaCl, 0.1 mM EDTA, 10 mM Na_2HPO_4, pH 6.5. (Panel A) Hyperchromicity profiles of (○) the control duplex at 178 μM, (▽) the control duplex at 8.3 μM, (●) the αT duplex at 184 μM, (▼) the αT duplex at 10.2 μM. Markers indicate every 5th point. (Panel B) CD spectra of (○) the control duplex at 9.6 μM, 10 °C, (▽) the control duplex at 9.6 μM, 85 °C, (●) the αT duplex at 9.6 μM, 10 °C, (▼) the αT duplex at 9.6 μM, 85 °C. Markers indicate every 50th point. (Panel C) CD spectra of the control (○) and αT (●) duplexes at 230 μM, 10 °C. Markers indicate every 50th point. (Panel D) Concentration dependence of the T_m for the αT duplex. (Panels E and F) Thermal denaturation curves for control (○) and αT (●) duplexes. Markers indicate every 10th point.

hairpin formation under these conditions is minimal for both decamers. The results of these spectrophotometric studies suggest that the presence of the α-anomeric bases in the duplex do not cause global structural perturbations.

Both decamers contain the *Eco*RI recognition sequence GAATTC. However, in the αT decamer T7 is an α-anomeric nucleotide that is in a parallel stranded orientation and flanked by unusual 3′−3′ and 5′−5′ linkages. Hence, the restriction endonuclease *Eco*RI would be expected to be inhibited by this modification of the recognition site. This was confirmed by gel electrophoretic analysis of the *Eco*RI digestion under conditions that favor duplex formation (*vide supra*), which showed that the control decamer is a substrate for *Eco*RI while the αT duplex is not digested (data not shown). This experiment, however, only addresses whether or not *Eco*RI is able to hydrolyze the αT decamer and cannot provide any information on the binding of the enzyme to this decamer. We have, therefore, set up *Eco*RI digestion conditions under which 30% of the control decamer is hydrolyzed, and upon addition of an equimolar amount of the αT decamer the amount of digestion decreases to 14%; when a 10-fold excess of the αT decamer is added, only traces of the control decamer are digested (data not shown). In contrast, neither the addition of equimolar, 10-fold, nor 100-fold excesses of a DNA duplex that does not contain an *Eco*RI site has any effect on the hydrolysis of the control decamer. These experiments demonstrate that although the αT decamer is not a substrate for *Eco*RI, it is still able to strongly interact with the enzyme, which is consistent with our hypothesis that the αT component in the decamer only causes a local perturbation.

Thermodynamic Properties of the Duplexes. In order to address the thermodynamic consequences of parallel stranded components in an antiparallel double helix, we have carried out thermal denaturation experiments on the control and αT decamers. In the case of the αT decamer we did observe a higher tendency for hairpin formation at low ionic strength, low strand concentrations, and elevated temperatures than for the control. This resulted in a complex melting behavior at low strand concentrations where the concentration-dependent melting of the duplex precedes the denaturation of the hairpin structure (Figure 3D). Duplex formation at

Table 1: Thermodynamic Data for the αT (d(GCGAAT-3′-3′-(αT)-5′-5′-CGC)$_2$) and Control (d(GCGAATTCGC)$_2$) Duplexes

	αT	control
T_m[a] (°C)	54.7 (0.3)	59.8 (0.1)
$\Delta H°$ (kJ mol^{-1})	330[b] (15)	343 (12)
$\Delta S°$ (kJ mol^{-1} K^{-1})	0.946 (0.021)	0.940 (0.033)

[a] Melting temperatures reported are for 30 μM total strand concentration. T_m's were determined in 400 mM NaCl, 0.1 mM EDTA, 10 mM Na_2HPO_4, pH 6.5. Each T_m is the average of 6 independent measurements. The absorbance was monitored at 275 and 290 nm. The values in parentheses indicate standard deviation of the measurements. Initial melting studies were recorded in 50 mM NaCl at 260 nm. Under these conditions we could observe the presence of both dimer and at higher temperatures also of the hairpin form for the αT decamer, complicating the quantitative evaluation of the melting profiles. By increasing both the salt and strand concentrations, the dimer form was preferentially stabilized. [b] The data reported are based on the concentration dependence of the T_m in the region where the enthalpy calculated from the fitting of the melting curve was constant and where the concentration dependence of the T_m was indicative of bimolecular melting (above 62.5 μM). The strand concentration was varied from 10 to 435 μM for the αT decamer and from 8 to 43 μM for the control.

low strand concentration and temperatures is supported by the concentration independence of the hyperchromicity and CD spectra discussed above (Figure 3A−C). The decisive evidence in favor of this comes from the observation that the imino proton spectra obtained at optical strand concentration correspond to that of the duplex at standard NMR concentrations (*vide infra*, Figure 5). In order to obtain thermodynamic data for the duplex form, we have selected conditions which favor the duplex structure. Under these conditions, the UV melting profiles of both the control and the αT decamers are reversible and concentration dependent, diagnostic of intermolecular duplex formation (Figure 3D−F). Thermodynamic data were obtained from curve fitting of the individual melting profiles to a bimolecular denaturation incorporating temperature-dependent absorbances of both pure helix and pure coil forms, as well as from the concentration dependence of the melting point within the concentration range in which duplex melting was evident. Both the T_m and $\Delta H°$ of the α-containing decamer are only a fraction lower than those observed for the control, demonstrating that the presence of two parallel stranded αT residues in this decamer duplex translates into only a small decrease in thermal stability (Table 1). We could not observe duplex formation in an oligonucleotide system that contained both β- and several α-anomeric T residues, the latter in an antiparallel orientation (Kalisch et al., unpublished results). This is in contrast to a recent report that an oligodeoxynucleotide nonamer containing a single α-anomeric adenine could form an antiparallel duplex with its complement that is comparable in stability to that for the unmodified sequence (Ide et al., 1995). On the basis of molecular modeling, these authors postulated that the αA can form two hydrogen bonds with a T, albeit in a reverse Watson−Crick manner. It is at present, however, unclear whether this is a unique property of an α-anomeric A and what the experimental structure is.

NMR Spectroscopy. *^{1}H NMR.* Inspection of the ^{1}H NMR spectra of the control and αT duplex decamers in D_2O, shown in Figure 4, reveals that the signals for the nonlabile protons in the two duplexes are highly homologous, particularly in the base proton and methyl regions. In both cases, no additional peaks due to the potential presence of a minor

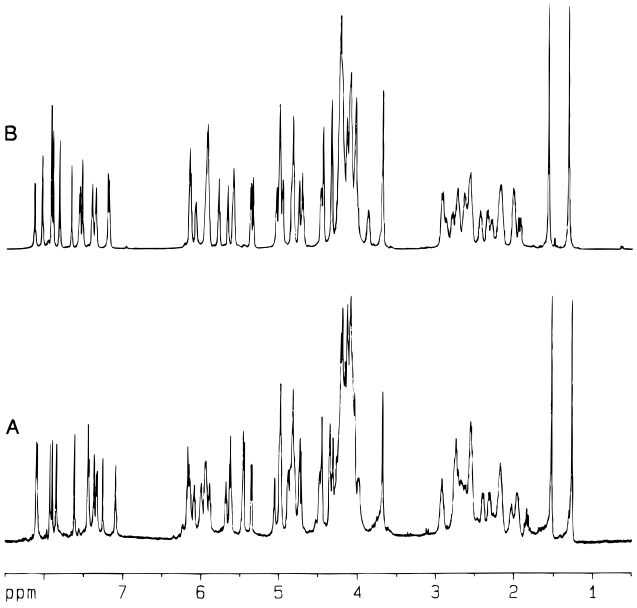

FIGURE 4: ^{1}H (600.1 MHz) NMR spectra of the decamers in D_2O. (A) d(GCGAATTCGC)$_2$, 2.6 mM, 303 K; (B) d(GCGAAT-3′-3′-(αT)-5′-5′-CGC)$_2$, 6.8 mM, 303 K.

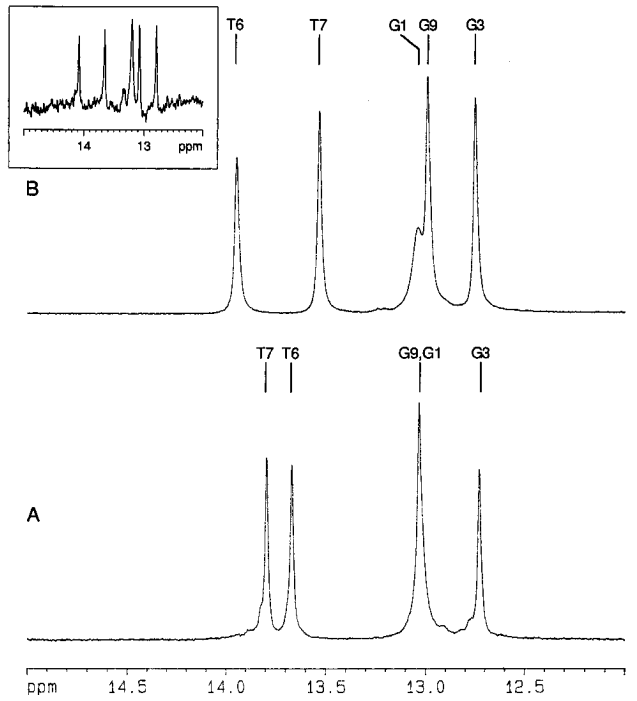

FIGURE 5: Imino proton region of the ^{1}H (600.1 MHz) NMR spectra of (A) d(GCGAATTCGC)$_2$ (2.6 mM) and (B) d(GCGAAT-3′-3′-(αT)-5′-5′-CGC)$_2$ (6.8 mM); 32 scans each, 293 K. Note that the imino proton signals for G1 and G9 in the parent decamer (A) are degenerate under these conditions. Inset: imino ^{1}H (600.1 MHz) spectrum of the αT decamer recorded at optical concentrations (1.2 OD_{260}/mL, corresponding to a duplex concentration of 6.0 μM; 10 mM Na_2HPO_4, 400 mM NaCl, 0.1 mM EDTA, pH 6.6, 280 K, 15 000 scans). The minor resonance(s) at $\delta \approx 13.35$ ppm are most likely due to a small percentage of hairpin form at this temperature.

hairpin form could be detected. The imino proton spectra of the duplexes obtained in water, with assignments obtained via 2D NOESY with jump and return, are shown in Figure 5. For both complexes, one observes resonances for each of the five chemically distinct base pairs, demonstrating the presence of stable base pairing and base stacking in the αT decamer. Although there are differences in the positions of

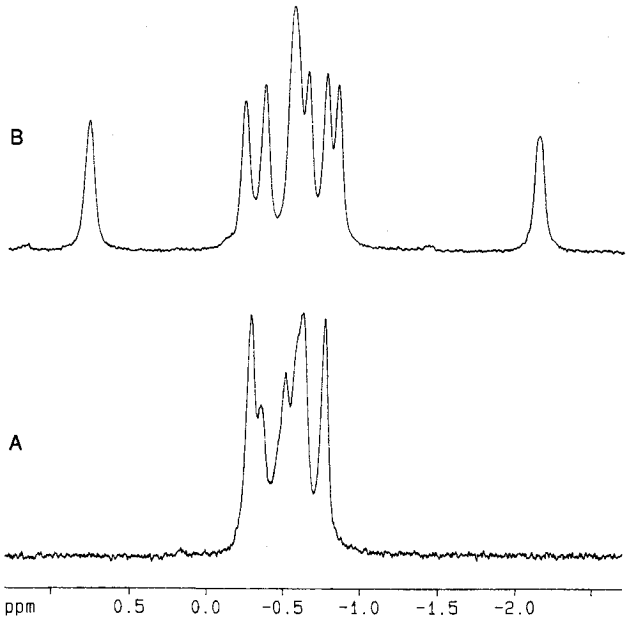

FIGURE 6: ^{31}P (242.9 MHz) NMR spectra of the decamers in D_2O. (A) d(GCGAATTCGC)$_2$, 2.6 mM, 303 K; (B) d(GCGAAT-3′-3′-(αT)-5′-5′-CGC)$_2$, 6.8 mM, 303 K.

the characteristically downfield shifted imino protons in the AT base pairs between the two samples, the chemical shifts of the guanosine imino protons are virtually identical. In addition, the temperature dependences of the imino proton resonances in both duplexes are also quite similar (data not shown).

^{31}P NMR. The established sensitivity of the ^{31}P chemical shift to changes in the conformation of the phosphodiester backbone has made ^{31}P NMR spectroscopy a powerful tool in the study of nucleic acids (Gorenstein, 1992). ^{31}P NMR spectra of d(GCGAATTCGC)$_2$ and d(GCGAAT-3′-3′-(αT)-5′-5′-CGC)$_2$ under identical conditions are shown in Figure 6. In the case of the control duplex, ^{31}P signals for all nine phosphorus atoms in the sequence resonate in a narrow chemical shift range ($\delta \approx -0.3$ to -0.8 ppm) that is diagnostic of right-handed B-DNA (Chen & Cohen, 1984). For the αT decamer, one observes overlapping ^{31}P signals due to seven phosphodiester bonds in virtually the same region of the spectrum ($\delta \approx -0.2$ to -0.8 ppm), in addition to signals downfield and upfield of these corresponding to the 5′−5′ and 3′−3′ linkages, respectively; similar trends in the ^{31}P data for these unusual linkages have been reported in the literature (Germann et al., 1989; Koga et al., 1995). Using ^{1}H-detected ^{31}P−^{1}H correlation spectroscopy (spectrum not shown) in combination with the elucidated ^{1}H resonances for the 3′ sugar protons (*vide infra*), we have assigned all nine ^{31}P signals for both duplexes (see Table 2) and have confirmed that the well-resolved resonances in the top spectrum are due to the unusual phosphodiester bonds in this decamer. The ^{31}P NMR results suggest that the insertion of one nucleotide into antiparallel stranded B-DNA in a parallel orientation does not impart substantial structural changes to the altered phosphodiester backbone in the α duplex other than at the 3′−3′ and 5′−5′ linkages.

Assignments of ^{1}H NMR Signals. Table 2 provides a list of ^{1}H (and ^{31}P) assignments in both duplexes obtained using standard two-dimensional techniques (Wüthrich, 1986). Briefly, DQF-COSY and TOCSY experiments on the duplexes in D_2O elucidated the intraresidue furanose ring spin systems from the H1′ to H4′, as well as the spin−spin connectivities between the cytosine base protons, H5 and H6, and the H6 and methyl groups in the two thymine bases (spectra not shown). Several H5′/5″ resonances were assigned using the ^{1}H-detected ^{31}P−^{1}H correlation approach alluded to above. Subsequently, NOE contacts linked sugar and base proton signals within each nucleotide and in a sequential manner (*vide infra*). The H2′ and H2″ sugar protons could be discriminated on the basis of intraresidue NOEs to nearby base (H6 in pyrimidines and H8 in purines) and H1′ protons. Note that, for an α-anomeric deoxyribose, H2″ is closer to H6/H8, while H2′ is juxtaposed to H1′; hence, for αT7 one finds that d_i(H6;2″) < d_i(H6;2′) and d_i-(1′;2′) < d_i(1′;2″), exactly opposite to the behavior of the β anomers.[2] Finally, the identities of H2 protons in the adenine bases were deduced from intraresidue (i.e., d_i(2;1′)) and interstrand base pair (i.e., d_{pi}(T3;A2)) NOE cross-peaks (data not shown).

Two sequential NOE connectivity networks linking base (H6/H8) and sugar proton (H1′ or H2′/H2″) resonances in a 5′ to 3′ direction highly diagnostic of regular right-handed B-DNA duplexes (Scheek et al., 1984; Wüthrich, 1986) facilitated the assignment of the nonlabile protons in both decamers. The pathways are as follows: (1) d_i(6,8;1′) → d_s(1′;6,8) → d_i(6,8;1′) → d_s(1′;6,8) ... etc.; (2) d_i(6,8;2′) → d_s(2″;6,8) → d_i(6,8;2′) → d_s(2″;6,8) ... etc. Figure 7 shows the H1′ and H2′/2″ to base regions of the NOESY (τ_m = 75 ms) spectrum of d(GCGAAT-3′-3′-(αT)-5′-5′-CGC)$_2$ in D_2O. For both duplexes one observes an uninterrupted flow of NOE contacts from H8 of G1 to H1′ of C10; this is illustrated for the αT duplex in the left panel of Figure 7. Notice the intense cross-peak between H1′ of αT7 and H6 of C8, reflecting the close proximity of these protons in the structure and resulting from the change in stereochemistry at the C1′ sugar position in αT7. Similarly, in the control duplex one also observes a continuous network of NOEs involving the H2′,H2″ and H6,H8 base protons (data not shown). However, in the α duplex, there is a break in the NOESY walk between H2′,H2″ of αT7 and H6 of C8 in the (right panel of Figure 7). A similar absence of sequential NOEs involving these sugar protons has been observed in the α-strands of α-β DNA hybrids (i.e., Gmeiner et al., 1992). In NOESY spectra obtained at longer mixing times (i.e., τ_m = 150−300 ms), an analogous disruption of the d_s(3′;6,8) connectivities also occurs at the same point in the α duplex (data not shown). The differences in the sequential sugar to base NOE connectivity patterns shown schematically in Figure 8 suggest that significant structural changes in the α duplex are restricted to the region encompassing the α-nucleotide.

In addition to the NOE pathways described above, a number of observations further illustrate that the global structures of the parent and αT decamers are very similar. First, it is apparent from Table 2 that significant chemical shift differences between resonances in the two duplexes are largely confined to the backbone (^{31}P) and sugar residues of

[2] The shorthand used in this paper to represent NOE contacts between two protons follows the convention given by Wüthrich (1986); i.e., for two nuclei A and B: d_i(A;B) denotes an intranucleotide distance; d_s(A;B) represents a sequential (same strand) contact between nonlabile protons, where A and B are in the 5′ and 3′ nucleotides, respectively; and d_{pi}(A;B) symbolizes an interstrand distance between protons within a base pair.

Table 2: ^{1}H and ^{31}P Resonance Assignments for d(GCGAAT-3′-3′-(αT)-5′-5′-CGC)$_2$ and d(GCGAATTCGC)$_2$[a]

	^{1}H NMR											
	H8	H2	H6	H5	H1′	H3′	H4′	H5′/H5″	H2′	H2″	CH_3	imino
						(a) αT Duplex						
G1	7.927				5.943	4.835	4.226	3.693	2.567	2.744		13.040
C2			7.359	5.344	5.605	4.832	4.149	4.098	2.015	2.347		
G3	7.822				5.598	5.003	4.336	4.013	2.648	2.801		12.751
A4	8.043	7.207			5.960	5.048	4.446	4.202	2.639	2.931		
A5	8.139	7.668			6.150	5.015	4.452	4.245	2.567	2.927		
T6			7.190		5.922	4.855	4.238	4.123	2.173	2.295	1.312	13.950
αT7			7.531		6.083	5.002	4.752	4.091	2.876	1.936	1.567	13.535
								3.876				
C8			7.566	5.671	5.788	4.720	4.199	nd	2.005	2.441		
G9	7.903				5.934	4.969	4.344	4.043	2.588	2.722		12.993
C10			7.404	5.375	6.161	4.481	4.041	4.228	2.176	2.176		
						(b) Control Duplex						
G1	7.926				5.949	4.822	4.210	3.682	2.554	2.744		13.031
C2			7.331	5.350	5.616	4.820	4.127	4.085	1.937	2.305		
G3	7.847				5.457	4.987	4.307	nd	2.654	2.749		12.727
A4	8.102	7.253			5.997	5.052	4.444	4.162	2.690	2.920		
A5	8.090	7.617			6.139	4.985	4.453	4.254	2.548	2.902		
T6			7.089		5.883	4.793	4.190	nd	1.960	2.540	1.262	13.671
T7			7.364		6.083	4.881	4.193	nd	2.152	2.533	1.523	13.795
C8			7.442	5.631	5.678	4.849	4.130	4.165	2.025	2.387		
G9	7.899				5.931	4.974	4.349	nd	2.611	2.718		13.031
C10			7.439	5.459	6.169	4.475	4.032	4.224	≈2.16	≈2.16		

	^{31}P NMR								
decamer	P1	P2	P3	P4	P5	P6	P7	P8	P9
αT	−0.54	−0.24	−0.77	−0.65	−0.84	−2.14	0.77	−0.57	−0.37
control	−0.57	−0.28	−0.50	−0.63	−0.77	−0.76	−0.61	−0.28	−0.35

[a] ^{1}H (600.1 MHz) and ^{31}P (242.9 MHz) NMR assignments for d(GCGAAT-3′-3′-(αT)-5′-5′-CGC)$_2$ and d(GCGAATTCGC)$_2$ in 50 mM NaCl, 10 mM phosphate buffer, pH 6.5 at 303 K (293 K for the imino protons). Initial assignment was based on standard DNA assignment strategies. However, utilizing inverse ^{31}P−^{1}H correlation experiments, the sequential assignments (H3′, H5′,5″, and H4′) were confirmed without any assumptions about the structure. In most cases only one of the protons on the C5′ carbon of the deoxyribose ring could be unambiguously assigned to a residue, due to resonance overlap; we have not discriminated between the two diastereotopic methylene protons (i.e., H5′ vs H5″) in our assignment. Imino proton signals were assigned using 1−1 NOESY experiments. nd, not determined.

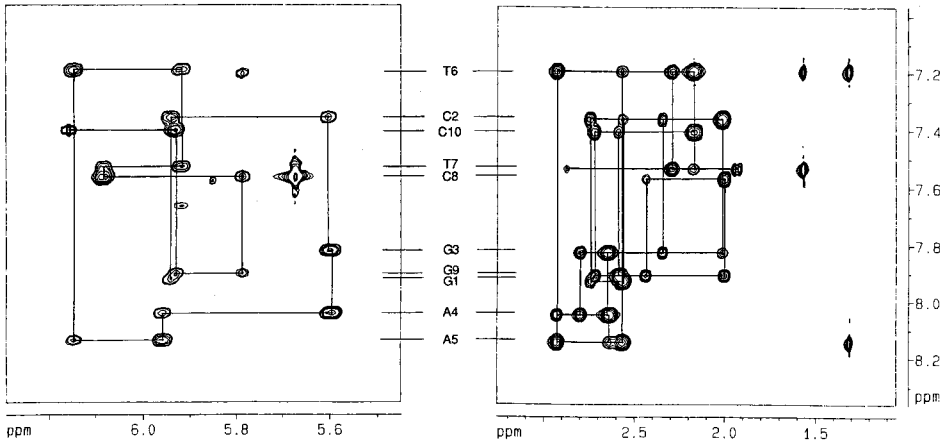

FIGURE 7: NOESY (τ_m = 75 ms) spectrum of d(GCGAAT-3′-3′-(αT)-5′-5′-CGC)$_2$ (6.8 mM) in D_2O, 303 K; 2.3 and 4.7 Hz/pt resolution in F2 and F1, respectively. Left: H6/8−H1′ region. Right: H6/H8−H2′/H2″ region.

the inverted nucleotide (αT7) and neighboring residues (i.e., C8), reflecting the change in configuration at the C1′ position in αT7 and the unusual phosphodiester linkages in its vicinity. This is particularly true for the H2′ and H2″ protons in αT7, which are substantially downfield and upfield, respectively, of the corresponding signals in the β-nucleotides in both strands. In addition, the signal for H4′ is also appreciably shifted to lower field; these effects have been noted in studies of α-β DNA hybrids (Lancelot et al., 1987). Second, a number of NOE connectivities diagnostic of right-handed B-DNA with the base in the anti conformation are preserved in the α duplex. For example, short contacts between the T methyl groups and the H6 or H8 protons of the base to the 5′ side of the each thymidine (i.e., d_s(6,8;M)) are observed for both decamers, indicating that the methyl groups of T6 and T7 are in the major groove, as expected for regular B-DNA with Watson−Crick base pairing (see right panel of Figure 7). In addition, within both duplexes,

[3] In the case of an α-anomeric sugar, the syn range is functionally equivalent to an anti conformation in β-nucleotides. This means that one observes the characteristic intraresidue NOE contacts normally found for β-nucleotides. Furthermore, the identical position of a sugar residue relative to the base in α and β anomers is given by the relation: $\chi_\alpha = \chi_\beta + 200°$ (Lancelot et al., 1989).

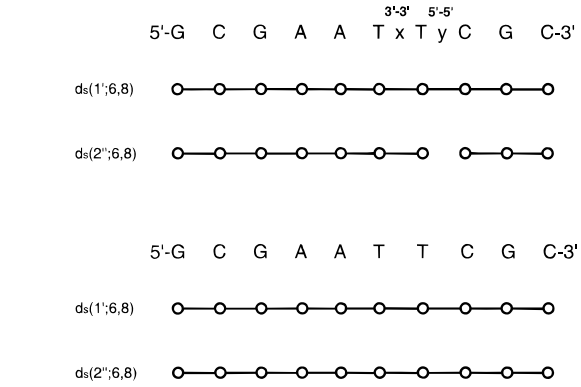

FIGURE 8: Schematic diagram showing the sequential $d_s(1';6,8)$ and $d_s(2'';6,8)$ NOESY connectivities (represented by open circles) for $d(GCGAATTCGC)_2$ and d(GCGAAT-3′-3′-(αT)-5′-5′-CGC)$_2$ (τ_m = 75 ms; D_2O).

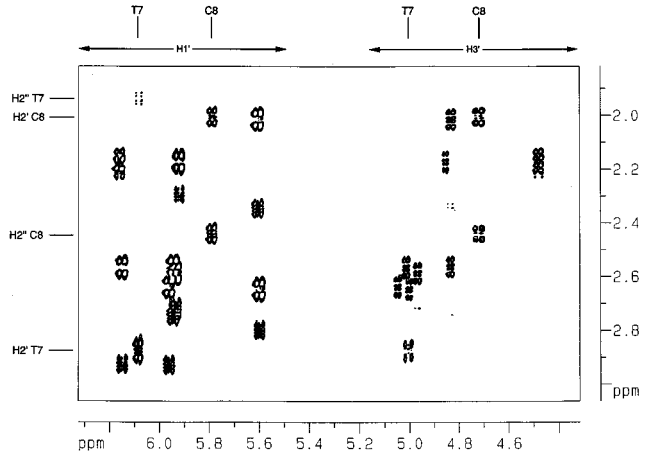

FIGURE 9: Portion of the DQF-COSY of d(GCGAAT-3′-3′-(αT)-5′-5′-CGC)$_2$ (6.8 mM) in D_2O, 303 K, showing H2′/H2″−H1′ and H2′/H2″−H3′ connectivities. The data were strip transformed to enhance spectral resolution in each dimension (0.59 and 1.17 Hz/pt in *F*2 and *F*1, respectively).

intraresidue H2′/H2″ to base H6/H8 NOE cross-peaks are much stronger than analogous H1′ to base proton contacts, meaning that all bases with the exception of αT7 are in the anti configuration.[3] A prominent $d_i(6;4')$ contact for αT7 further establishes the orientation of the base in this nucleotide (Lancelot et al., 1987; Gmeiner et al., 1992). The properties of the H2 adenine base protons are also quite comparable in the two duplexes and highly diagnostic of right-handed B-DNA. In both cases, one can observe NOE cross-peaks between the H2 protons of consecutive adenines (i.e., $d_s(2;2)$) (data not shown). Furthermore, the T_1 values (in D_2O at 303 K) of these protons are extremely long in both complexes (control: A4: 6.1 s; A5: 5.3 s; α: A4: 4.9 s; A5: 5.3 s), in contrast to their relaxation properties in, for example, parallel stranded DNA (Germann et al., 1995).

Sugar Ring Puckering. Spin−spin coupling constants between neighboring furanose protons, derived from phase-sensitive homonuclear correlation spectroscopy, provide insight into the conformations of the sugar rings in nucleic acids (Wijmenga et al., 1993; van Wijk et al., 1992). An expansion of the DQF-COSY of the α duplex, containing the H1′ and H3′ to H2′/H2″ regions, is shown in Figure 9. For several nucleotides in the sequence (i.e., G1 to T6, and G9), one observes the classic multiplet patterns for the H1′/H2′ and H1′/H2″ cross-peaks expected for B-DNA, in which the sugar adopts a C2′-endo, or S-, pucker. For these residues we find that $^3J_{1'2'} + {}^3J_{1'2''}$ range from ≈14.7 to 15.9 Hz with $^3J_{1'2'} > {}^3J_{1'2''}$ ($^3J_{1'2'} \approx 9.4-10.6$ Hz; $^3J_{1'2''} \approx 4.7-5.3$ Hz). In addition, couplings between H2″ and H3′ are nearly or completely absent; these traits are consistent with S-type sugar puckering. Similar data were obtained for the resolvable signals (i.e., G1 through G9) in the control duplex decamer studied (data not shown). With the sums of the H1′ coupling constants (∑1′) in hand, one can gain insight into the nature of the conformational exchange between the N- and S-type sugar puckerings in β-deoxyribose nucleic acids, using the equation (Rinkel & Altona, 1987):

$$f_s = \frac{\sum 1' - 9.8}{5.9} \qquad (2)$$

where f_s represents the mole fraction of the S-type conformer for a given nucleotide in the sequence. The data above correspond to a greater than 83% population of the S-form for these residues and are consistent with those of Rinkel et al. (1987a) for a virtually identical self-complementary decamer $d(CCGAATTCGG)_2$; in that case, the conformational equilibria for the sugar rings in all ten residues were also reported to be highly skewed toward the S-type conformer (70−100%). However, the coupling patterns for the αT7 and C8 furanose ring protons in the αT decamer are noticeably different. For these nucleotides, the sum of the $^3J_{1'2'} + {}^3J_{1'2''}$ is substantially lower (12.5−12.9 Hz). In the case of the α sugar, $^3J_{1'2'}$ remains larger than $^3J_{1'2''}$ (8.2 and 4.7 Hz, respectively), and one observes no coupling between the H2″ and H3′. In accordance with previous NMR studies of α-β DNA hybrids (Gmeiner et al., 1992), these data suggest that this sugar adopts an S-type conformation, but the amplitude of the puckering is reduced. The lack of a significant N-type contribution to the conformation of this α-anomeric sugar is further substantiated by the very weak $d_i(1';3')$ and $d_i(2'';4')$ NOE contacts observed at a mixing time of 30 ms (data not shown). Both of these cross-peaks are predicted to be significantly larger if this residue spends any appreciable time in an N-type conformation. For C8, $^3J_{1'2''}$ is actually larger than $^3J_{1'2'}$ (7.6 and 5.3 Hz, respectively) and there is a coupling between H2″ and H3′. These data suggest an increase in N-character for the puckering in this sugar (≈50% using eq 2). This view is corroborated by the presence of a somewhat larger $d_i(2'';4')$ NOE cross-peak (τ_m = 30 ms) detected for this residue, compared to others in the molecule (data not shown), which is diagnostic of a shift in the pseudorotation angle toward the Northern hemisphere (Wüthrich, 1986).

Model of the α *Duplex Decamer.* A portion of a model of the αT decamer duplex containing the alpha nucleotide and adjacent base pairs is shown in Figure 10. The model, generated by QUANTA and AMMP, is qualitatively in agreement with our spectroscopic data on several grounds. First, the model is consistent with the finding that the local inversion of the strand polarity at the αT position enables this nucleotide to form a regular Watson−Crick base pair with the A residue on the complementary strand; furthermore, this parallel base pair snugly fits into the helix while maintaining the base stacking. Second, the bases are in the anti orientation, with the exception of αT7. This residue is formally in the syn range; however, the H6−H1′ distance is similar to that observed for β anomeric nucleotides in anti conformation (Lancelot et al., 1989).[3] Third, the observed

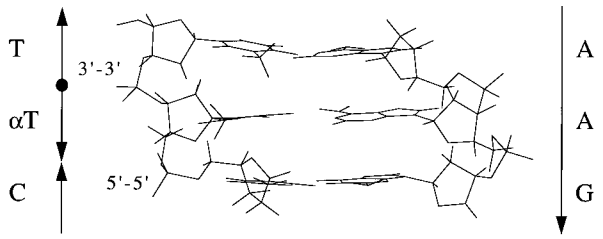

FIGURE 10: Model of a region in the αT decamer duplex encompassing the α-anomeric nucleotide as well as the 3′−3′ and 5′−5′ phosphodiester linkages. The arrows indicate the sequence polarity. Note that the sugar puckering for each nucleotide in the model shown is of the S-type; this is valid for all residues including C8, which has an equal probability of adopting N- and S-conformations (see text).

H1′/H6,8 and H2′,H2″/H6,8 NOE pathways are consistent with the corresponding distances in this model; in particular, the H1′/base NOESY walk can be followed throughout the entire sequence, whereas H2′,H2″/base NOE pathway breaks down between αT7 and C8. This model is currently being further refined using relaxation matrix methods (Borgias & James, 1989) and ^{31}P-derived NMR experiments to investigate the backbone conformation of the unusual linkages.

CONCLUSIONS

As alluded to in the opening remarks of this paper, antisense oligonucleotides should ideally possess the following properties: (1) form a stable duplex structure with a specific target RNA sequence; (2) cellular uptake; (3) nuclease resistance; and (4) RNase H activity (i.e., of the RNA strand in the RNA−DNA hybrid).

In practice, it has proven difficult to combine these desirable traits in one antisense oligonucleotide. Although purely α-anomeric antisense nucleotides can form stable structures with their targets and are not degraded by nucleases, the resulting complexes are RNase H resistant. However, recent studies demonstrate that it is possible to generate potential antisense oligonucleotides which contain α- and β-anomeric components (for example, a β core flanked by α-anomeric tracts) and possess all the traits listed above (van de Sande et al., 1994; Kalisch et al., unpublished results; Boiziau et al., 1995). Consequently, it is vital to have a grasp of the thermodynamic and structural parameters of the modifications within such sequences in order to rationally design more potent antisense oligodeoxynucleotides. The results presented in this study establish the structural and thermodynamic properties of an oligonucleotide containing inverted anomeric centers and strand polarity reversals; the latter were accomplished via 3′−3′ and 5′−5′ phosphodiester linkages. In spite of the presence of these unusual components, our results demonstrate that the self-complementary decamer is capable of forming a stable duplex. Based on enzymatic and spectroscopic data, we conclude that, in the case of an αT nucleotide, structural changes are confined to the α-anomeric nucleotides and residues in its immediate proximity. Moreover, the α-anomeric nucleotide fits remarkably well into a double helical DNA structure, despite the fact that the presence of a single α is actually rather taxing, since, in contrast to the case of an extended stretch of α-anomeric nucleotides, two distinct structural junctions are created within a pre-existing helix. We are currently analyzing the properties of analogous sequences containing the α-isomers of A, C, and G with the goal of gaining insight into the sequence-dependent thermostability, and structures, of such constructs. A natural progression from this work is to examine the more physiologically relevant hybrids of such α-containing DNA strands with their RNA complements.

ACKNOWLEDGMENT

We are indebted to Dr. Robert Harrison (Thomas Jefferson University) for his assistance in modeling studies using the AMMP program.

REFERENCES

Bax, A., & Davis, D. G. (1985) *J. Magn. Reson. 65*, 355−360.
Bertrand, J. R., Imbach, J.-L., Paoletti, C., & Malvy, C. (1989) *Biochem. Biophys. Res. Commun. 164*, 311−318.
Boiziau, C., Kurfurt, R., Cazanave, C., Roig, V., Thuong, N. T., & Toulmé, J.-J. (1991) *Nucleic Acids Res. 19*, 1113−1119.
Boiziau, C., Thuong, N. T., & Toulmé, J.-J. (1992) *Proc. Natl. Acad. Sci. U.S.A. 89*, 768−772.
Boiziau, C., Debart, F., Rayner, B., Imbach, J-L., & Toulmé, J.-J. (1995) *FEBS Lett. 361*, 41−45.
Borgias, B. A., & James, T. L. (1989) *Methods Enzymol. 176*, 169−183.
Cantor, C. R., & Schimmel, P. R. (1980) *Biophysical Chemistry*, Freeman and Co., San Francisco, CA.
Chaconas, G., & van de Sande, J. H. (1980) *Methods Enzymol. 65*, 75−85.
Chen, C.-W., & Cohen, J. S. (1984) in *Phosphorus-31 NMR Principles and Applications* (Gorenstein, D., Ed.) pp 233−263, Academic Press, Orlando, FL.
Crooke, S. T. (1993) *FASEB J. 7*, 533−539.
De Mesmaeker, A., Häner, R., Martin, P., & Moser, H. E. (1995) *Acc. Chem. Res. 28*, 366−374.
Derome, A., & Williamson, M. (1990) *J. Magn. Reson. 88*, 177−185.
Germann, M. W., Pon, R. T., & van de Sande, J. H. (1987) *Anal. Biochem. 165*, 399−405.
Germann, M. W., Kalisch, B. W., & van de Sande, J. H. (1988) *Biochemistry 27*, 8302−8306.
Germann, M. W., Vogel, H. J., Pon, R. T., & van de Sande, J. H. (1989) *Biochemistry 28*, 6220−6228.
Germann, M. W., Zhou, N., van de Sande, J. H., & Vogel, H. J. (1995) *Methods Enzymol. 261*, 207−225.
Gmeiner, W. H., Rao, K. E., Rayner, B., Vasseur, J.-J., Morvan, F., Imbach, J.-L., & Lown, J. W. (1990) *Biochemistry 29*, 10329−10341.
Gmeiner, W. H., Rayner, B., Morvan, F., Imbach, J.-L., & Lown, J. W. (1992) *J. Biomol. NMR 2*, 275−288.
Gorenstein, D. G. (1992) *Methods Enzymol. 211*, 254−286.
Guesnot, J.-L., Vovelle, F., Thuong, N. T., & Lancelot, G. (1990) *Biochemistry 29*, 4982−4991.
Harrison, R. W. (1993) *J. Comput. Chem. 14*, 1112−1122.
Harrison, R. W., & Weber, I. T. (1994) *Protein Eng. 7*, 1353−1363.
Hélène, C. (1994) *Eur. J. Cancer 30A*, 1721−1726.
Ide, H., Shimizu, H., Kimura, Y., Sakamoto, S., Makino, K., Glackin, M., Wallace, S. S., Nakamuta, H., Sasaki, M., & Sugimoto, N. (1995) *Biochemistry 34*, 6947−6955.
Jacob, A., Duval-Valentin, G., Ingrand, D., Thuong, N. T., & Hélène, C. (1993) *Eur. J. Biochem. 216*, 19−24.
Koga, M., Wilk, A., Moore, M. F., Scremin, C. L., Zhou, L., & Beaucage, S. L. (1995) *J. Org. Chem. 60*, 1520−1530.
Lancelot, G., Guesnot, J.-L., Roig, V., & Thuong, N. T. (1987) *Nucleic Acids Res. 15*, 7531−7547.
Lancelot, G., Guesnot, J.-L., & Vovelle, F. (1989) *Biochemistry 28*, 7871−7878.
Lavignon, M., Tounekti, N., Raynor, B., Imbach, J.-L., Keith, G., Paoletti, J., & Malvy, C. (1992) *Antisense Res. Dev. 2*, 315−324.
Marion, D., & Wüthrich, K. (1983) *Biochem. Biophys. Res. Commun. 113*, 967−974.

Marky, L. A., Blumenfeld, K. S., Kozlowski, S., & Breslauer, K. J. (1983) *Biopolymers 22*, 1247−1257.
Milligan, J. F., Matteucci, M. D., & Martin, J. C. (1993) *J. Med. Chem. 36*, 1923−1937.
Morvan, F., Rayner, B., Imbach, J.-L., Lee, M., Hartley, J. A., Chang, D.-K., & Lown, J. W. (1987) *Nucleic Acids Res. 15*, 7027−7044.
Paoletti, J., Bazile, D., Morvan, F., Imbach, J.-L., & Paoletti, C. (1989) *Nucleic Acids Res. 17*, 2693−2704.
Plateau, P., & Guéron, M. (1982) *J. Am. Chem. Soc. 104*, 7310−7311.
Praseuth, D., Chassignol, M., Takasugi, M., Le Doan, T., Thuong, N. T., & Hélène, C. (1987) *J. Mol. Biol. 196*, 939−942.
Ramsing, N. B., & Jovin, T. M. (1988) *Nucleic Acids Res. 16*, 6659−6676.
Rinkel, L. J., & Altona, C. (1987) *J. Biomol. Struct. Dyn. 4*, 621−649.
Rinkel, L. J., van der Marel, G. A., van Boom, J. H., & Altona, C. (1987a) *Eur. J. Biochem. 163*, 275−286.
Rinkel, L. J., van der Marel, G. A., van Boom, J. H., & Altona, C. (1987b) *Eur. J. Biochem. 163*, 287−296.
Rippe, K., & Jovin, T. M. (1992) *Methods Enzymol. 211*, 199−220.
Scheek, R. M., Boelens, R., Russo, N., van Boom, J. H., & Kaptein, R. (1984) *Biochemistry 23*, 1371−1376.
Séquin, U. (1973) *Experimentia 29*, 1059−1062.
Sklenar, V., & Bax, A. (1987) *J. Magn. Reson. 74*, 469−479.
Sklenar, V., Miyashiro, H., Zon, G., Miles, T., & Bax, A. (1986) *FEBS Lett. 208*, 94−98.
Stein, C. A., & Cheng, Y.-C. (1993) *Science 261*, 1004−1012.
Thuong, N. T., Asseline, U., Roig, V., Takasugi, M., & Hélène, C. (1987) *Proc. Natl. Acad. Sci. U.S.A. 84*, 5129−5133.
van de Sande, J. H., Ramsing, N. B., Germann, M. W., Elhorst, W., Kalisch, B. W., Pon, R. T., Clegg, R. C., & Jovin, T. M. (1988) *Science 241*, 551−557.
van de Sande, J. H., Kalisch, B. W., & Germann, M. W. (1990) in *Molecular Basis of Specificity in Nucleic Acid-Drug Design Interactions* (Pullman, B., and Jortner, J., Eds.), pp 261−274, Kluwer Academic Publishers, The Netherlands.
van de Sande, J. H., Kalisch, B. W., Quong, B. Q., & Germann, M. W. (1994) Antisense Oligonucleotides with Polarity and Anomeric Center Reversal. First International Antisense Conference of Japan, Kyoto, Dec 4−7.
van Wijk, J., Huckriede, B. D., Ippel, J. H., & Altona, C. (1992) *Methods Enzymol. 211*, 287−306.
Vichier-Guerre, S., Pompon, A., Lefebvre, I., & Imbach, J.-L. (1994) *Antisense Res. Dev. 4*, 9−18.
Wagner, R. W. (1994) *Nature 372*, 333−335.
Weber, I. T., & Harrison, R. W. (1996) *Protein Eng.* (in press).
Weiner, S. J., Kollman, P. A., Nguyen, D. T., & Case, D. A. (1986) *J. Comput. Chem. 7*, 230−252.
Westhof, E. (1987) *J. Biomol. Struct. Dyn. 5*, 581−600.
Wijmenga, S. S., Mooren, M. M. W., & Hilbers, C. W. (1993) in *NMR of Macromolecules; A Practical Approach* (Roberts, G. C. K., Ed.) pp 217−288, Oxford University Press, New York.
Wüthrich, K. (1986) *NMR of Proteins and Nucleic Acids*, John Wiley & Sons, New York.
Zelphati, O., Imbach, J.-L., Signoret, N., Zon, G., Rayner, B., & Leserman, L. (1994) *Nucleic Acids Res. 22*, 4307−4314.
Zhou, N., Germann, M. W., van de Sande, J. H., Pattabiraman, N., & Vogel, H. J. (1993) *Biochemistry 32*, 646−656.

BI960612P